Flow Science Report 01-12

Modeling Turbulent Entrainment of Air at a Free Surface

C.W. Hirt 5/24/12
Flow Science, Inc.

Overview

In free-surface flows the turbulence in the liquid may be sufficient to disturb the surface to the point of entraining air into the flow. This process is important, for example, in water treatment where air is needed to sustain microorganisms for water purification and in rivers and streams for sustaining a healthy fish population. Air entrainment is typically engineered into spillways downstream of hydropower plants to reduce the possibility of cavitation damage at the base of the spillway. Situations where air entrainment is undesirable are in the sprue and runner systems used by metal casters, and in the filling of liquid containers used for consumer products.

The importance of being able to predict the amount and distribution of entrained air at a free liquid surface has led to the development of a unique model in ***FLOW-3D***®. The model has two options. One option, to be used when the volume fraction of entrained air is relatively low, uses a passive scalar variable to record and transport the air volume fraction. This model is passive in that it does not alter the dynamics of the flow.

The second air-entrainment model option is based on a variable density formulation. This model includes the "bulking" of fluid volume by the addition of air and the buoyancy effects associated with entrained air. This dynamically coupled model cannot, however, be used in conjunction with heat transport and natural (thermal) convection.

In addition, when using the variable density formulation, the model can include a relative drifting of air in water, the possible escape of air if it rises to the surface of the water and the removal or addition of air to trapped bubble regions represented as adiabatic bubbles.

The same basic entrainment process is used in both options. It is based on a competition between the stabilizing forces of gravity and surface tension and the destabilizing effects of surface turbulence.

Because turbulence is the main cause of entrainment, a turbulence-transport model must be used in connection with the air-entrainment model. It is recommended that the RNG version of the more traditional k-epsilon turbulence model be employed. All the validation tests reported in this Technical Note were performed using the RNG model.

Using the Model

There are two ways that this entrainment model may be used. For small amounts of entrained air a scalar variable is defined to record the fractional volume of entrained air. In this simple model, entrained air does not change the volume or density of the liquid. This is a reasonable approximation as long as the fractional volume of entrained air f_a remains small. To insure that the volume fraction of air does not exceed unity in this

version of the model, which would make no sense and could cause computational troubles, air entrainment stops at volume fraction of air of 0.9 or larger.

A second way to employ the air entrainment model is to use the one-fluid, variable density option. In this case the volume of entrained air is taken into account as an increase in the total fluid (mixture) volume fraction. Furthermore, buoyancy effects associated with a variable mixture density are also taken into account.

The amount of entrained air as defined by its volume fraction is simply the value of the scalar variable when that version of the model is used. With the variable density model version the volume fraction, f_a, of air can be computed from the relation

$$\rho=(1-f_a)\text{rhof}+f_a\text{rhofs},$$

where ρ is the mixture density output by the program. When rhofs/rhof << 1 (e.g.., air/water=0.001), then a good approximation is $f_a=(\text{rhof}-\rho)/\text{rhof}$.

A scalar function is still used with the variable density option where it records the volume fraction of air as computed from the density. Displays are then made directly for air concentrations without having to convert the mixture density.

Validation of the Model

Four different tests have been conducted to validate the usefulness of the air-entrainment model. For all cases we have simply used a constant entrainment coefficient $C_{air}=0.5$ and the properties of water and air.

Jet into a Pool

An axisymmetric jet of water of diameter 1 cm is allowed to fall under gravity into a pool of stationary water that is 3 cm deep. The jet begins its fall 4 cm above the surface of the pool. The jet velocity where it enters the pool is approximately 1.0 m/s (100 cm/s).

Experimental data (Ervine 1980) indicates that there is a critical jet velocity of about 0.8 m/s below which no air entrainment will occur. Alternative experimental data of Chanson, et al (2004) suggests that the critical jet velocity is closer to 1.58 m/s. As our simulation tests will show, the amount of turbulence in a jet, which may be thought of as perturbations in the experiments, has a strong influence on the amount of air entrained. It is our belief that there is no absolute "critical velocity" for entrainment, but rather there is an upper limit on jet velocity that depends on the level of turbulence inherent in the jet: the smoother the jet the greater the "critical velocity" before entrainment begins.

In the computational model, if no turbulence is included in a simulation (i.e., no turbulence models are used) there is no entrainment as shown in Fig.1a. Actually a small amount of entrainment does occur but this is very small, less than 0.003%. This result and all others displayed in Fig.1 have used the passive model of air entrainment because of the relatively small amount of air being entrained.

Physically, some fluid turbulence is expected when a jet enters a pool because of the large velocity shears that occur at the intersection. This is accounted for in our simulations by including an RNG turbulence transport model. As a result there is some small amount of air entrained, Fig.1b. The entrainment is intermittent and is associated with some sloshing of the pool surface interacting with the jet. At about one jet diameter below the pool surface the average volume fraction of air is computed to be less than 0.01%.

These results seem quite reasonable, but to put it in perspective it is useful to see what the entrainment is when the jet is additionally given some initial turbulence energy. For example, if the jet has an initial 2% level of turbulence (i.e., $0.02*U^2/2$, where U=0.2 m/s is the average velocity of the jet at the inlet to the computational region) then the simulation shows an approximate average 8% volume of air at one jet diameter below the surface, Fig.1c. There are large fluctuations in this value from 1% to 19%, again because of the sloshing of the pool caused by the impinging jet.

Clearly, the level of turbulence in the jet, even when small, has a significant influence on the entrainment of air. This may explain why different experiments have seemingly found different "critical velocities" for jets.

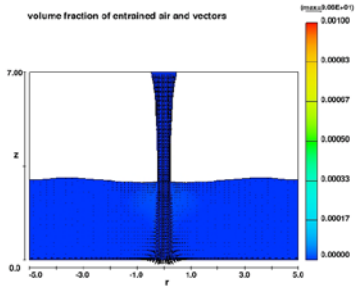

Fig.1a. Computed air entrained without turbulence.

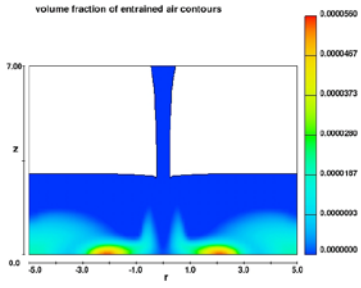

Fig.1b. Air entrained with turbulence model, but zero jet turbulence.

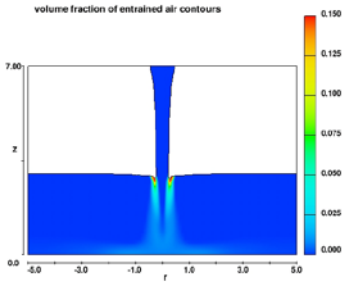

Fig.1c. Air entrained with 2% turbulence in the jet.

No data for the spatial distribution of entrained air in the pool has been found with which to make comparisons. However, the general level of entrainment of 8% below the pool surface with 2% turbulence in the jet seems quite reasonable (see the next example).

Drop Shaft

A problem closely related to a jet into a pool is that of water flowing into a vertical shaft. In this case we have simulated experimental data obtained by Ervine (1981) for rectangular, vertical drop shafts. Because the shaft was rectangular it is possible to use a two-dimensional model that corresponds to a vertical section of the shaft. In our case the shaft has a width of 0.5 m and a depth of 2.0 m. The bottom end of the shaft is open and immersed in water with a pressure head of 1.0 m. Only the right half of the top of the shaft is open to the flow of water, which has an average velocity of 1.56 m/s.

Water enters the top and falls under gravity as a wall jet along the right side of the shaft. The pool height in the shaft is unsteady, it moves up and down about the center of the shaft (i.e., 1.0 m above the bottom). The width of the jet where it enters the pool is about 0.08 m and has a vertical velocity of about 4.5 m/s, which corresponds to a Froude number of roughly Fr=5.7.

The simulation employed the variable density model because it was thought that buoyancy caused by air entrainment might have some effect on the flow in the pool. Repeating the simulation with the passive option showed little difference in the results, presumably because the jet velocity is so large that buoyancy forces cannot compete with inertia, at least in the region modeled.

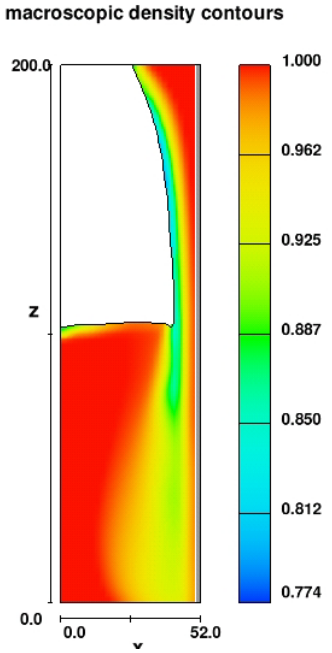

Figure 2a. Variable density in drop shaft flow indicates air entrainment.

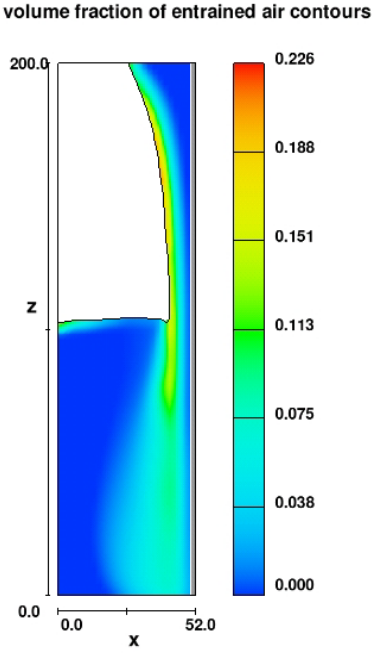

Figure 2b. Volume fraction of air entrainment in the drop shaft.

As already noted, the flow does not reach a steady state, but exhibits an oscillation in pool height, with discrete eddies generated by the jet moving downward and out the bottom of the shaft. A snapshot of the computed flow shown in Fig.2a provides a good picture of the general distribution of mixture (air/water) density. The concentration of air is shown in Fig.2b.

Ervine (1981) measured the ratio of the volumetric flow of air to that of water, Q_a/Q_w, and gives the empirical correlation,

$$\frac{Q_a}{Q_w} = 0.0045 Fr^2 \left(1 - \frac{u_c}{u_{jet}}\right)^3, \qquad with \quad u_c = 0.8 \quad m/s.$$

For the simulated case u_{jet}=4.5 m/s and Fr=5.7, so that the empirical result should be Q_a/Q_w=0.081. To get volumetric flow rate data from the simulation a code addition was made to compute and print the ratio of volume flow rate for air versus that for water.

In any case, the computed results give a mean value of Q_a/Q approximately equal to 0.070, close to the experimental result of 0.081. The computed value exhibited an oscillation of about ±10% because of the unsteadiness of the flow. However, the experimental data are reported to have an accuracy of ±20% in relation to the corresponding empirical equation. The computed values are thus seen to be in good agreement with the data for both the passive and variable density models.

As in the previous example of a plunging jet, the amount of turbulence in the incoming flow has a strong influence on the amount of air that is entrained. For the results shown in Fig.2 the inlet turbulence level is 1.5%, based on the inlet velocity of 1.56 m/s.

A series of simulations were repeated using a range of inlet turbulence levels and the resulting values of Q_a/Q_w are shown in Table 1. Clearly, in order to accurately predict the amount of air entrainment in this example it is necessary to have a good idea of the amount in turbulence initially contained in the inflow stream. By the same token, if the idea of the shaft flow device is to entrain lots of air to remove it from the shaft then introducing a flow disturbance at the inlet will significantly aid in achieving this goal.

Inlet Turbulence Level %	Computed Q_a/Q_w
1.0	0.024
1.33	0.049
1.5	0.070
2.0	0.176

Hydraulic Jump in a Conduit

The third test case involves a closed conduit. In this case the conduit is inclined 5.71 degrees (10% slope) with respect to the horizontal. The lower end of the conduit is immersed in water whose hydrostatic head at the top edge of the outlet is 0.0612 m. At the inlet, water enters with a depth of 0.05 m. and rushes down the conduit under the action of gravity. A hydraulic jump develops about 0.5 m downstream from the inlet.

For simplicity the circular conduit is modeled with a two-dimensional vertical slice through its center. The conduit has a diameter of 0.15 m. and a length of 1.0 m. The variable density model option with drift and air escape was used for the simulation, and no turbulence was added to the inlet flow.

Figure 3 shows snapshots of the computed result at the end of the simulation, t=8.0 s. There is some small unsteadiness associated with the hydraulic jump, as there should be, but the average flow is nearly steady.

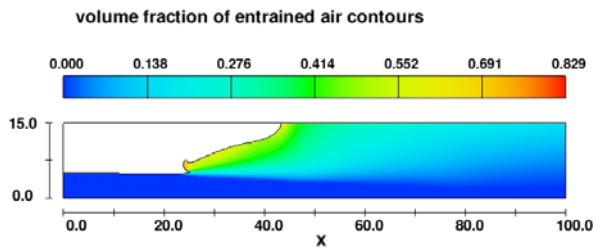

Figure 3. Hydraulic jump in the conduit. Color indicates volume fraction of air.

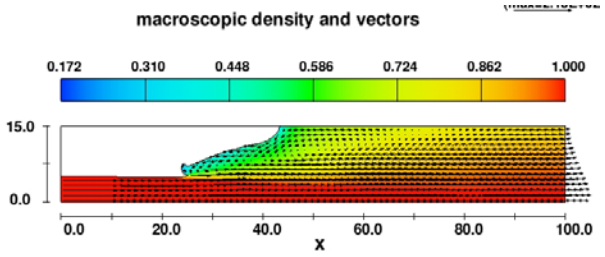

Figure 3b. Hydraulic jump in the conduit. Density and every other vector plotted. Note a recirculation region at front of jump.

This test case was designed to approximate an experimental study reported by Kalinske and Robertson ("Closed Conduit Flow,", by Kalinske, A.A. and Robertson, J.M., published paper in an unknown Symposium proceedings is based on doctoral work of Robertson submitted to the U. of Iowa August, 1941).

The relevant data obtained in the experimental study are the air-to-water volumetric flow rate ratios versus the Froude number (Fr) of the incoming flow. The data is represented by the empirical expression,

$$\frac{Q_a}{Q_w} = 0.0066(Fr - 1)^{1.4}$$

For the case simulated the Froude number was 3.0 and the average computed ratio of flow rates is 0.055, which is to be compared to the above formula's value of 0.0174. The computational result is higher, which should perhaps be expected because the model only considers the 2D midsection of the conduit. In any case the amount of air entrained and carried downstream is relatively small in both the experiment and simulation. In contrast, the amount of air in the recirculation region at the front of the jump is much larger.

Spillway

The final test involves a model spillway for which there is considerable experimental data for a range of slopes and flow rates. The experimental data is reported in Wood 1991 and is a summary of experimental work conducted by L.G. Straub and A.G. Anderson of the St. Anthony Falls Hydraulics Laboratory at the U. of Minnesota, 1958.

The experiments involved a straight sloped chute arranged at various angles with respect to the horizontal and with a gate at the top end that could be used to set the flow rate down the chute. Detailed measurements were made of the amount of air entrained at the end of the model spillway as a function of depth. It was assumed that the distribution at the end of the modeled spillway reached an observed "equilibrium" condition where it was no longer varying significantly with distance along the spillway surface. This example, in contrast to all the previous examples, does not involve a plunging flow of one fluid stream into another.

The case chosen for simulation has been taken from Wood's Figure 3.20. A flat chute has a slope of 37.5° and a flow rate of 0.929 m^3/s/m (i.e., 0.929 m^3/s for each meter of width across the chute, which is assumed to closely approximate a two-dimensional flow situation). The chute is defined in a rectangular region 18 m long, which is 2.75 m longer than that of the experiments, 1 m wide and 0.3 m in depth. The floor of the chute has a roughness of 0.001 m corresponding to concrete. The size of the grid elements in the vertical direction are 0.015 m, resulting in about 8 elements covering the terminal depth of flow.

The variable density entrainment model with drift and gas escape was used for this simulation in order to have the most realistic model possible. In the experiments the free surface of the water flow was taken to be at a volume fraction of air of 0.9. To conform to this the two-phase drift-flux model was assigned a minimum allowed water fraction of 0.1, and the air entrainment model has a cutoff for entrainment when the air volume fraction reaches 0.9.

To simulate the slope of 37.5° the gravity vector was tilted so that there was a component of gravity directed down the chute. At the inlet to the chute a velocity of 4.645 m/s was specified, but flow was blocked by a baffle above a height of 0.215 m, which gives the desired flow rate.

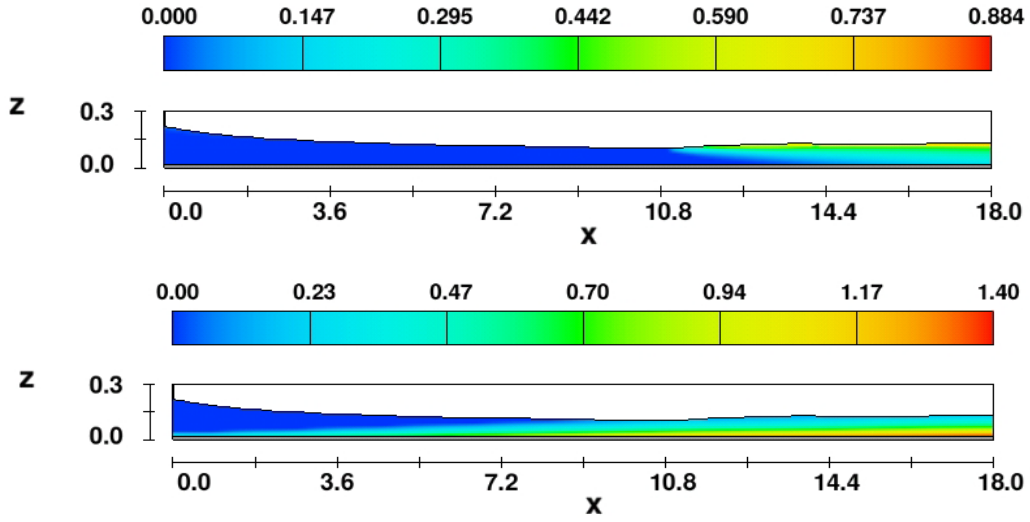

Figure 4. Entrained volume fraction of air (top) and turbulent kinetic energy (bottom).

Figure 4 shows-steady state results computed for this arrangement; Fig.4 top frame is the distribution of air volume fraction and Fig.4 bottom frame is that of the turbulent kinetic energy. It will be seen that air is not entrained until turbulence has reached the free surface. A close inspection of the change in surface height also shows that bulking is occurring because of the entrained air. Near the bottom (right) end of the flow it appears that conditions are not changing much with distance along the chute, which supports the experimental observation that an "equilibrium" has been reached. However, if we enlarge the last meter of the computed flow, Fig.5, it can be seen that there is still some

small changes in the volume fraction of air, which should be expected for physical reasons. The changes, however, are small and probably below the sensitivity of the physical measurements.

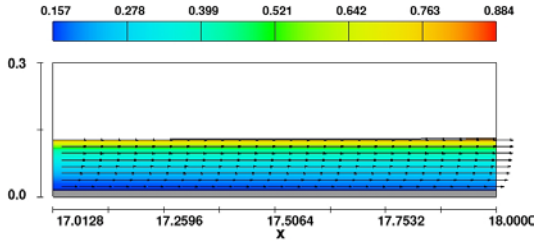

Figure 5. Volume fraction of air and velocity vectors in the last 1 m of the model spillway. Very slight changes are seen with respect to distance along the spillway.

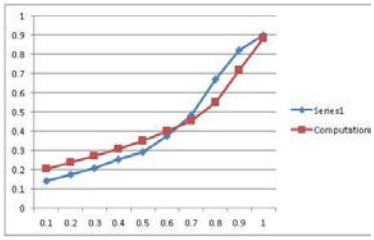

Figure 6. Comparison experimental data (blue) and computational results (red) for air entrainment volume fraction (vertical axis) versus the normalized depth (x-axis).

A comparison of the measured and computed air volume fraction distribution versus depth at the end of the model spillway is shown in Fig.6. There is some discrepancy in the shape, but the overall level of agreement is quite good. To make this plot the computed data were linearly interpolated to lie at uniform intervals of the normalized depth.

Summary

An air entrainment model has been incorporated into ***FLOW-3D***®. The model can be used with one of two options. For low air volume fractions a simple passive scalar function is used to record the amount of entrained air. When higher volume fractions of air are likely, or when the buoyancy of the air/water mixture is important, a second model option can be used that records entrained air in terms of a variable mixture density.

For either model option there is one empirical parameter, C_{air}, a nondimensional coefficient that can be adjusted, but the recommended value of C_{air}=0.5 was found to work well for all the test cases considered. Changes from the recommended value should only be made when there is irrefutable evidence to justify the change.

Four different types of sample problems were used to test the new model and good results were obtained in every case. The most sensitive aspect in all the simulations was found to be the level of turbulence in the impinging flow that entered a pool of liquid. This sensitivity does not occur in situations where the entrainment is associated with a hydraulic jump because in those cases the instability of the jump generally over shadows any initial turbulence. Nor does it occur in situations such as a spillway where the entrainment arises from turbulence generated by the flow over a roughened surface.

Acknowledgements
The author wishes to thank Mr. Fabian Bombardelli at the U. of Illinois and Dr. Jim Dexter of INCA Engineering, Inc. for their encouragement to undertake this model development and especially for their efforts to locate suitable data with which to perform the validation tests.

References
1980 Ervine, D.A., McKeogh, E., and Elsawy, E.M., "Effect of turbulent intensity on the rate of entrainment by plunging water jets," Proc. Inst. Civil Engrs., June, pp.425-455.

1981 Ervine, D.A., McKeogh, E., and Elsawy, E.M., "Model prototype conformity in hydraulic structures involving aeration," Proc. XIXth IAHR Congress, New Delhi, India, Vol. 5, Feb. 1981, pp.s65-72.

2004 Chanson, H., Aoki, S. and Hoque, A., "Physical Modeling and Similitude of Air-Bubble Entrainment at Vertical Circular Plunging Jets," Chem. Eng. Sci., **59**, p747.

1991 Wood, I.R., "Air Entrainment in Free Surface Flows," IAHR Monograph, "Hydraulic Design Considerations," published by Balkema, Rotterdam.